

Generative Semantic Communications with Foundation Models: Perception-Error Analysis and Semantic-Aware Power Allocation

Chunmei Xu, *Member, IEEE*, Mahdi Boloursaz Mashhadi, *Senior Member, IEEE*, Yi Ma, *Senior Member, IEEE*, Rahim Tafazolli, *Fellow, IEEE*, Jiangzhou Wang, *Fellow, IEEE*

Abstract—Generative foundation models can revolutionize the design of semantic communication (SemCom) systems by enabling high fidelity exchange of semantic information at ultra-low rates. In this work, a generative SemCom framework utilizing pre-trained foundation models is proposed, where both uncoded forward-with-error and coded discard-with-error schemes are developed for the semantic decoder. Using the rate-distortion-perception theory, the relationship between regenerated signal quality and transmission reliability is characterized, which is proven to be non-decreasing. Based on this, semantic values are defined to quantify the semantic similarity between multimodal semantic features and the original source. We also investigate semantic-aware power allocation problems that minimize power consumption for ultra-low rate and high fidelity SemComs. Two semantic-aware power allocation methods are proposed by leveraging the non-decreasing property of the perception-error relationship. Based on the Kodak dataset, perception-error functions and semantic values are obtained for image tasks. Simulation results show that the proposed semantic-aware method significantly outperforms conventional approaches, particularly in the channel-coded case (up to 90% power saving).

Index Terms—Semantic communication, generative foundation model, rate-distortion-perception, semantic-aware power allocation.

I. INTRODUCTION

Communication systems have been developed and optimized based on Shannon information theory over the past decades, achieving remarkable success. However, the focus is primarily on the accurate reconstruction of a source signal rather than the underlying meaning of the source content. A new paradigm called semantic communication (SemCom) has emerged, shifting focus to precise content reconstruction with equivalent semantics [1, 2]. SemCom demonstrates significant potential for achieving ultra-low compression rates and enhanced resource efficiency, maintaining effectiveness even when partial information is lost under semantic metrics.

This work was supported by the U.K. Department for Science, Innovation, and Technology under Project TUDOR (Towards Ubiquitous 3D Open Resilient Network).

C. Xu, M. Boloursaz Mashhadi, Y. Ma and, R. Tafazolli are with 5GIC & 6GIC, Institute for Communication Systems (ICS), University of Surrey, Guildford, U.K. (emails: {chunmei.xu; m.boloursazmashhadi; y.ma; r.tafazolli}@surrey.ac.uk).

J. Wang is with the School of Engineering, University of Kent, CT2 7NT Canterbury, U.K. (e-mail: j.z.wang@kent.ac.uk).

Since the establishment of Shannon’s information theory, researchers have pursued the development of semantic information theory through various approaches. Initial efforts characterized semantic information by introducing semantic entropy concept using logical probability [3] and fuzzy mathematics theory [4, 5]. Theoretical advances emerged through rate-distortion theory, examining semantic information properties via intrinsic state pairs [6] and joint probability distributions [7]. A recent development came with Niu *et al.*’s systematic framework for semantic information theory, which developed novel semantic entropy measures and comprehensive theorems in semantic source, channel, and rate-distortion coding [8]. Furthermore, the authors in [9] introduced a new conceptualization of SemCom, and formulated two fundamental problems termed language exploitation and language design, aiming to shed light on the intricate dynamics of SemCom. It is also recognized that semantic information should be task-dependent, corresponding to specific tasks or goals at the destination [2]. This insight motivates the integration of rate-distortion-perception theory [10] into SemCom, providing a theoretical framework to analyze source encoding efficiency in capturing semantic information while maintaining perceptual quality performance. Despite these advances, a universal semantic information theory for SemCom system design remains an open challenge.

Nevertheless, the rapid advancement of artificial intelligence (AI) has enabled significant progress in the SemCom systems, particularly through deep learning approaches. The deep learning-enabled SemCom typically employs an end-to-end architecture to jointly learn the neural network (NN)-based semantic encoder and decoder, establishing a shared knowledge base between transceivers. The deep joint source and channel coding (JSCC) proposed in [11] adopted auto-encoder NN networks for image tasks, sparking numerous deep JSCC variants for various types of sources and channel models [12–15]. To train a deep JSCC model, the loss function was generally designed based on measurable distortion metrics such as mean square error (MSE) and peak-signal-to-noise (PSNR). While these deep JSCC approaches demonstrate superior performance compared to conventional separated source and channel coding schemes, they fundamentally adhere to Shannon’s rate-distortion theory due to the use

of the distortion-based loss functions. However, distortion of SemCom systems may no longer serve as the key performance indicator for emerging applications with specific tasks or goals, where accurate semantic information conveying becomes the primary objective.

Generative SemCom systems, utilizing deep generative AI models such as variational autoencoder (VAE), generative adversarial network (GAN), and diffusion model, show promise in preserving semantics while reducing data traffic [16]. In [17], the authors proposed a VAE-based deep JSCC system that optimizes compression rate and error correction simultaneously, achieving robust data representations and competitive performance against conventional separated schemes. At receivers, the adopted GANs were trained using sophisticated loss functions, which combined the MSE and perceptual distances in [18], and incorporated reconstruction, synchronization and binary discriminator errors in [19]. More recently, state-of-art diffusion models have achieved breakthrough in image [20], audio [21], and video [22] generation tasks, offering stronger stability than GAN models in synthesizing multimedia content while preserving semantics. A generative diffusion-guided SemCom framework was proposed, where the loss function was designed as the weighted sum of the MSE and Kullback-Leibler (KL) divergence [23]. This diffusion-guided SemCom was shown to achieve high robustness to extremely bad channel conditions and superior performance in generating semantically equivalent images.

However, the above deep learning-enabled SemCom systems face two challenges in their end-to-end architecture. Firstly, analog modulations are required for gradient computation and back-propagation during training, which conflicts with modern digital communication systems. Secondly, training semantic encoders and decoders for fading and noisy channels demands substantial computational resources while showing poor generalization across different data sources and channel models. To address these, a potential solution is to adopt foundation models like bidirectional encoder representations from transformers (BERT) and generative pre-trained transformer (GPT). These models, trained on vast amounts of diverse datasets, can capture general patterns and thereby enable knowledge base sharing between transceivers. Particularly promising are the generative foundation models based on diffusion models, such as DALL-E and Sora, which can synthesize high perceptual quality signals by exchanging extremely compressed textual prompts. These advances motivate to design SemCom systems using foundation models, conveying semantic information with minimal data traffic.

In this work, we propose a generative SemCom framework that uses pre-trained foundation models for semantic encoding and decoding. With semantic encoder and decoder fixed, transmission reliability emerges as the key factor affecting the perceptual quality of regenerated signals. We analyze their relationship through rate-distortion-perception theory

and develop semantic-aware resource allocation strategies to optimize power consumption while maintaining semantic performance. For the ultra-low rate and high fidelity SemCom, we focus on high-reliability schemes: uncoded binary phase shift keying (BPSK) for channel-uncoded case and finite block length coding [24] for channel-coded cases respectively. The main contributions of this work are summarized as follows:

- A generative SemCom framework is proposed using pre-trained foundation models as semantic encoder and decoder, leveraging their shared knowledge bases and generalization capabilities without additional training. Both uncoded forward-with-error and coded discard-with-error schemes are developed in the semantic decoder.
- The relationship between transmission reliability and regenerated signal quality is analyzed through rate-distortion-perception theory, proving that perception value deteriorates with transmission errors. Semantic values of transmitted and received data streams are defined based on the perception value to quantify their semantic similarities with the original source.
- The semantic-aware power allocation problems under both channel-uncoded and channel-coded cases are investigated to minimize total power consumption while maintaining the semantic performance. Two methods are developed by leveraging the non-decreasing property of the perception-error relationship.
- Perception-error functions and semantic values under both uncoded forward-with-error and coded discard-with-error schemes are obtained through simulations on the Kodak dataset. Compared to conventional approaches, the proposed semantic-aware bisection method achieves power savings of up to 10% and 90% in channel-uncoded and channel-coded cases, respectively.

II. GENERATIVE SEMCOM FRAMEWORK

This section introduces the proposed generative SemCom framework as depicted in Fig. 1, which consists of semantic encoder, transmission scheme, and semantic decoder.

A. Semantic Encoder

The semantic encoder employs I semantic extractors to extract semantic features from the inputted source signal \mathbf{X} using the pre-trained foundation models $F_{\text{enc},i}$. The i -th semantic feature can be expressed by

$$\mathbf{S}_i = F_{\text{enc},i}(\mathbf{X} | \theta_i^*), \quad (1)$$

where θ_i^* is the NN parameters of the i -th foundation model. For image signals, these semantic features may include prompts, edge maps and segmented semantics, extracted using various pre-trained models such as image-to-text transformers [25], [26], the Holistically-nested Edge Detection (HED) model [27] and the DeepLab model [28], respectively. To ensure compatibility with existing digital communication systems, each semantic feature \mathbf{S}_i is converted into a bit

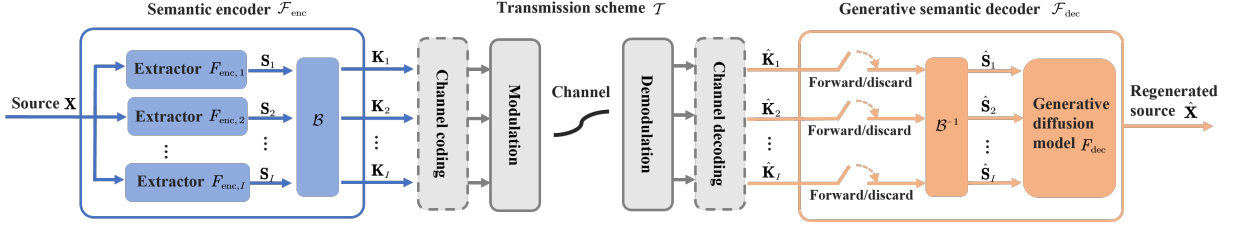


Fig. 1. The proposed generative semantic communication framework with pre-trained foundation models.

sequence, termed a semantic data stream \mathbf{K}_i , through the operation $\mathbf{K}_i = \mathcal{B}(\mathbf{S}_i)$, where $\mathcal{B}(\cdot)$ is the binary mapping function such as ASCII, Unicode, and quantization.

Each semantic data stream contributes differently to the perceptual quality of the regenerated signal when evaluated under a specific semantic metric, which is highly related to the inference goal or task at the destination. This makes it fundamentally different from conventional communication systems that equally treat all data streams. To quantify the contribution of each data stream, we introduce the semantic value L_i to characterize its semantic similarity with the original source signal (defined in the Sec. III-C). A larger L_i indicates that the i -th data stream has a greater impact on the perpetual quality of the regenerated signal, implying that it is more important.

B. Transmission Scheme

In the proposed generative SemCom framework, the multi-stream transmission is modeled as:

$$[\hat{\mathbf{K}}_1, \hat{\mathbf{K}}_2, \dots, \hat{\mathbf{K}}_I] = \mathcal{T}([\mathbf{K}_1, \mathbf{K}_2, \dots, \mathbf{K}_I]), \quad (2)$$

where $\mathcal{T}(\cdot)$ is the transmission scheme that maps from the transmitted data streams to the received ones, which encompasses channel coding, modulation, demodulation, and channel decoding. These data streams are transmitted orthogonally to eliminate the inter-stream interference.

Due to the fading and noisy effects of the wireless channels, the received semantic data stream $\hat{\mathbf{K}}_i$ may contain errors. The probability of receiving $\hat{\mathbf{K}}_i$ is denoted as $\mathbb{P}(\hat{\mathbf{K}}_i | \mathbf{K}_i; \mathcal{T})$, which depends on the bit error rate (BER) ψ_i (≤ 0.5) in the channel-uncoded case. The block error rate (BLER) of the i -th semantic data stream is denoted as $\Psi_i = \mathbb{P}(\hat{\mathbf{K}}_i \neq \mathbf{K}_i; \mathcal{T})$. While hybrid automatic repeat request (HARQ) mechanisms can ensure correct transmission, they introduce additional latency. Alternatively, the transmission reliability can be improved by adopting adaptive coding and modulation schemes based on channel conditions.

C. Generative Semantic Decoder

At the generative semantic decoder, signal regeneration is performed using the received data streams $\hat{\mathbf{K}}_i$. To handle transmission errors, we propose two distinct processing

schemes: uncoded forward-with-error scheme for channel-uncoded case and coded discarded-with-error scheme for channel-coded case. This differentiation arises because transmission errors in channel-uncoded cases cannot be detected, while channel-coded cases experience burst errors due to codeword correlation. These burst errors may even degrade performance (demonstrated in Fig. 5 in Sec. VI).

For uncoded forward-with-error scheme, all received semantic data streams $\hat{\mathbf{K}}_i$ are first reconverted into semantic features $\hat{\mathbf{S}}_i = \mathcal{B}^{-1}(\hat{\mathbf{K}}_i)$, where $\mathcal{B}^{-1}(\cdot)$ is the inverse operation of $\mathcal{B}(\cdot)$. These features are then forwarded to the generative foundation model F_{dec} to synthesize the generated signal $\hat{\mathbf{X}}$, expressed as

$$\hat{\mathbf{X}} = F_{\text{dec}}(\hat{\mathbf{S}}_1, \hat{\mathbf{S}}_2, \dots, \hat{\mathbf{S}}_I; \omega^*) \triangleq F_{\text{dec}}(\hat{\mathbf{K}}_{\mathcal{I}}), \quad (3)$$

where ω^* represents the NN parameters of the generative model, and $\hat{\mathbf{K}}_{\mathcal{I}} \triangleq \{\hat{\mathbf{K}}_i, i \in \mathcal{I}\}$ is the concatenated received data streams. For the coded discard-with-error scheme, semantic data streams containing errors are discarded to mitigate the impact of burst errors. Letting \mathcal{I}_c denote the index set of error-free received semantic data streams, the regenerated signal $\hat{\mathbf{X}}$ is expressed as

$$\hat{\mathbf{X}} = F_{\text{dec}}(\{\mathbf{S}_j\}_{j \in \mathcal{I}_c}; \omega^*) \triangleq F_{\text{dec}}(\mathbf{K}_{\mathcal{I}_c}), \quad (4)$$

where $\mathbf{K}_{\mathcal{I}_c} \triangleq \{\mathbf{K}_j, j \in \mathcal{I}_c\}$. The semantic decoder does not synthesize any signal when $\mathcal{I}_c = \emptyset$.

Within the proposed generative SemCom framework, the semantic information of the semantic data streams is lossy due to transmission errors. This implies that the semantic values of received data streams are reduced, i.e., $\hat{L}_{i,\text{forward}} \leq L_i$ and $\hat{L}_{i,\text{discard}} \leq L_i$. Here, $\hat{L}_{i,\text{forward}}$ and $\hat{L}_{i,\text{discard}}$ are the semantic values of the i -th semantic data stream $\hat{\mathbf{K}}_i$ under uncoded forward-with-error and coded discard-with-error schemes, respectively.

III. PERCEPTION-ERROR ANALYSIS AND SEMANTIC VALUE

This section characterizes how transmission errors affect the perceptual quality of the regenerated signal through rate-distortion-perception theory. Based on the analyzed perception-error relationship, the semantic values of the transmitted and received semantic data streams are defined to quantify their semantic similarity with the original source.

A. Rate-Distortion-Perception Function

The rate-distortion-perception theory [10][29], an extension of Shannon's rate-distortion theory, incorporates perceptual distance as an additional constraint. This theory examines three key metrics between the source signal \mathbf{X} and constructed signal $\hat{\mathbf{X}}$: rate (quantified by mutual information), distortion (measured by distortion distance), and perception (evaluated by perceptual distance). The rate-distortion-perception trade-off, which minimizes mutual information subject to distortion and perception constraints, is formulated as:

$$R(D, P) \triangleq \min_{P_{\hat{\mathbf{X}}|\mathbf{X}}} I(\mathbf{X}; \hat{\mathbf{X}}) \quad (5a)$$

$$\text{s.t. } \mathbb{E}[d(\mathbf{X}, \hat{\mathbf{X}})] \leq D \quad (5b)$$

$$\delta(P_{\mathbf{X}}, P_{\hat{\mathbf{X}}}) \leq P, \quad (5c)$$

where $P_{\mathbf{X}}$ and $P_{\hat{\mathbf{X}}}$ denote the distributions of the source signal \mathbf{X} and regenerated signal $\hat{\mathbf{X}}$ respectively, and $P_{\hat{\mathbf{X}}|\mathbf{X}}$ represents their conditional distribution. The measurable distortion function $d(\mathbf{X}, \hat{\mathbf{X}})$, typically designed as the squared error, is constrained by D .

$\delta(P_{\mathbf{X}}, P_{\hat{\mathbf{X}}})$ represents the perceptual distance constrained by P . It can be implemented using the distribution-based metrics such as KL divergence and Wasserstein distance [10][29]. As an alternative, $\delta(P_{\mathbf{X}}, P_{\hat{\mathbf{X}}})$ can be designed as non-distribution-based perceptual distances using the contrastive language-image pre-training (CLIP) similarity [30] or multi-scale structural similarity (MS-SSIM) [31], which are expressed as:

$$\delta(P_{\mathbf{X}}, P_{\hat{\mathbf{X}}}) \triangleq 1 - \mathbb{E}[\text{CLIP}(\mathbf{X}, \hat{\mathbf{X}})], \quad (6)$$

$$\delta(P_{\mathbf{X}}, P_{\hat{\mathbf{X}}}) \triangleq 1 - \mathbb{E}[\text{MS-SSIM}(\mathbf{X}, \hat{\mathbf{X}})], \quad (7)$$

where $\text{CLIP}(\mathbf{X}, \hat{\mathbf{X}})$ and $\text{MS-SSIM}(\mathbf{X}, \hat{\mathbf{X}})$ represent the CLIP and MS-SSIM similarity functions.

The CLIP similarity is obtained using the CLIP NN model that jointly trains image and text encoders to embed both modalities into a shared, high-dimensional feature space where semantically similar content clusters together [32]. Using contrastive learning on paired image-text data, it learns to maximize cosine similarity between matching pairs while minimizing it for non-matching pairs. Denoting the learned model F_{clip} with NN parameters θ_{clip} , the CLIP similarity function can be expressed as:

$$\text{CLIP}(\mathbf{X}, \hat{\mathbf{X}}) = \frac{F_{\text{clip}}(\mathbf{X}; \theta_{\text{clip}}) \cdot F_{\text{clip}}(\hat{\mathbf{X}}; \theta_{\text{clip}})}{\|F_{\text{clip}}(\mathbf{X}; \theta_{\text{clip}})\| \|F_{\text{clip}}(\hat{\mathbf{X}}; \theta_{\text{clip}})\|}, \quad (8)$$

where $\|\cdot\|$ is the ℓ_2 norm. The resulting score ranges from -1 to 1, with higher values indicating stronger semantic similarity. In addition, the MS-SSIM is widely used for image quality assessment in image processing and computer vision. $\text{MS-SSIM}(\mathbf{X}, \hat{\mathbf{X}})$ evaluates the perceptual similarity between the source signal \mathbf{X} and the reconstructed signal $\hat{\mathbf{X}}$ by analyzing luminance, contrast and structure across multiple scales. The final MS-SSIM score combines these components

using weighted products, yielding a value between 0 and 1, where 1 indicates perfect perceptual similarity and 0 indicates no structural similarity. Note that when no signal is regenerated (denoted as $\hat{\mathbf{X}}_{\emptyset}$), the CLIP and MS-SSIM similarities satisfy $\text{CLIP}(\mathbf{X}, \hat{\mathbf{X}}_{\emptyset}) = 0$ and $\text{MS-SSIM}(\mathbf{X}, \hat{\mathbf{X}}_{\emptyset}) = 0$.

B. Perception-Error Analysis

SemComs aim to convey the semantic meanings with minimal semantic loss, i.e., the smallest perceptual distance, regardless of distortion. Since distortion is not constrained in this context, we can set $D = \infty$ and reformulate the rate-distortion-perception trade-off in (5) as:

$$P(R) \triangleq \min_{P_{\hat{\mathbf{X}}|\mathbf{X}}} \delta(P_{\mathbf{X}}, P_{\hat{\mathbf{X}}}) \quad (9a)$$

$$\text{s.t. } I(\mathbf{X}; \hat{\mathbf{X}}) \leq R, \quad (9b)$$

which aims to find the conditional distribution $P_{\hat{\mathbf{X}}|\mathbf{X}}$ under the rate constraint R . In the proposed generative SemCom framework, $P_{\hat{\mathbf{X}}|\mathbf{X}}$ is jointly determined by the semantic encoder, transmission scheme, semantic decoder, and the channel conditions. Since the semantic encoder \mathcal{F}_{enc} and generative semantic decoder \mathcal{F}_{dec} are designed using pre-trained foundation models, only the transmission scheme \mathcal{T} and channel influence the regenerated signal's perceptual quality. This means that $P_{\hat{\mathbf{X}}|\mathbf{X}}$ depends solely on the conditional distribution $P_{\hat{\mathbf{K}}_{\mathcal{I}}|\mathbf{K}_{\mathcal{I}}}$ under the proposed generative SemCom framework.

The inputted source signal, transmitted data streams, received data streams, and generated signal form a Markov chain such that $\mathbf{X} \rightarrow \mathbf{K}_{\mathcal{I}} \rightarrow \hat{\mathbf{K}}_{\mathcal{I}} \rightarrow \hat{\mathbf{X}}$. Applying the data-processing inequality [33] yields two inequalities: $I(\mathbf{X}; \hat{\mathbf{X}}) \leq I(\mathbf{X}; \hat{\mathbf{K}}_{\mathcal{I}})$ and $I(\mathbf{X}; \hat{\mathbf{K}}_{\mathcal{I}}) \leq I(\mathbf{K}; \hat{\mathbf{K}}_{\mathcal{I}})$. These two inequalities combine to give:

$$I(\mathbf{X}; \hat{\mathbf{X}}) \leq I(\mathbf{K}_{\mathcal{I}}; \hat{\mathbf{K}}_{\mathcal{I}}). \quad (10)$$

The right-hand side of (10) further satisfies:

$$I(\mathbf{K}_{\mathcal{I}}; \hat{\mathbf{K}}_{\mathcal{I}}) \leq \sum_{i \in \mathcal{I}} I(\mathbf{K}_i; \hat{\mathbf{K}}_i), \quad (11)$$

where the equality holds if and only if the semantic data streams are independent. Combining (10) and (11) yields:

$$I(\mathbf{X}; \hat{\mathbf{X}}) \leq \sum_{i \in \mathcal{I}} I(\mathbf{K}_i; \hat{\mathbf{K}}_i). \quad (12)$$

By replacing (9b) with (12), problem (9) can then be approximated by:

$$P(R) \triangleq \min_{P_{\hat{\mathbf{K}}_{\mathcal{I}}|\mathbf{K}_{\mathcal{I}}}} \delta(P_{\mathbf{X}}, P_{\hat{\mathbf{X}}}) \quad (13a)$$

$$\text{s.t. } \sum_{i \in \mathcal{I}} I(\mathbf{K}_i; \hat{\mathbf{K}}_i) \leq R, \quad (13b)$$

where $P_{\hat{\mathbf{K}}_{\mathcal{I}}|\mathbf{K}_{\mathcal{I}}} = \prod_{i \in \mathcal{I}} P_{\hat{\mathbf{K}}_i|\mathbf{K}_i}$ due to the independent transmission of all data streams. The objective is to find the optimal conditional distribution $P_{\hat{\mathbf{K}}_{\mathcal{I}}|\mathbf{K}_{\mathcal{I}}}$ that minimizes the

perceptual distance, termed as the perception value, subject to the rate constraint R .

Lemma 1. *The perception-rate function $P(R)$ is non-increasing with rate R .*

Proof. The perception-rate function $P(R)$ represents the minimum perceptual distance achievable over a feasible set of conditional distributions $P_{\hat{\mathbf{K}}_{\mathcal{X}}|\mathbf{K}_{\mathcal{X}}}$. As R increases, this feasible set monotonically expands, and consequently, $P(R)$ is a non-increasing function of R . \square

The conditional distribution $P_{\hat{\mathbf{K}}_{\mathcal{X}}|\mathbf{K}_{\mathcal{X}}}$ is determined by both transmission schemes and channel conditions, naturally motivating the study of adaptive SemComs with channel feedback. However, simply combining conventional adaptive techniques with the generative SemCom might not offer additional semantic performance gains. This is because semantic features may exhibit varying levels of importance. Conventional adaptive techniques without considering semantic importance can assign less-important features to good channel conditions, resulting in inefficient uses of radio resources. This interesting problem invokes a new research direction in the scope of generative SemCom. This work is, however, focused on the generative SemCom with fixed coding rate, and investigate how transmission reliability affects the perceptual quality of the regenerated signal. To establish their relationship, we introduce the following assumption.

Assumption 1. *The bits within transmitted semantic data streams are assumed to be independent. The j -th bit of the i -th semantic data stream, denoted as \mathbf{K}_{ij} , follows a Bernoulli distribution with probability ϕ_{ij} of being 1 and $1 - \phi_{ij}$ of being 0. The probability Φ_i of sequence \mathbf{K}_i is given by $\Phi_i = \prod_{j=1}^{K_i} (\mathbf{K}_{ij}\phi_{ij} + (1 - \mathbf{K}_{ij})(1 - \phi_{ij}))$.*

Lemma 2. *Under Assumption 1, The mutual information between \mathbf{K}_i and $\hat{\mathbf{K}}_i$ for both the uncoded forward-with-error and coded discard-with-error schemes are given by:*

$$I(\mathbf{K}_i; \hat{\mathbf{K}}_i) = \sum_{j=1}^{K_i} H(\phi_{ij}) - H(\psi_{ij}), \quad (14)$$

and

$$I(\mathbf{K}_i; \hat{\mathbf{K}}_i) = H(\Phi_i) - \Psi_i H(\Phi_i), \quad (15)$$

respectively, where $H(\cdot)$ is the entropy function. The mutual information $I(\mathbf{K}_i; \hat{\mathbf{K}}_i)$ decreases with increasing BER ψ_{ij} or BLER Ψ_i . The proof is provided in Appendix A.

It is challenging to obtain the optimal distribution due to its dependence on source distribution $P_{\mathbf{X}}$ and the implicit mapping of pre-trained foundation models $F_{\text{enc},i}$ and F_{dec} . According to Assumption 1 and Lemma 2, finding the optimal solution for $P_{\hat{\mathbf{K}}|\mathbf{K}}$ becomes equivalent to optimizing the transmission scheme \mathcal{T} based on the channel conditions to obtain the optimal BER ψ_{ij} or BLER Ψ_i . For any rate R , there exists a corresponding optimal distribution solution

$P_{\hat{\mathbf{K}}_{\mathcal{X}}|\mathbf{K}_{\mathcal{X}}}$ (or equivalent optimal BER ψ_{ij} and BLER Ψ_i). Consequently, we can reframe the perception-rate function as a perception-error function to better characterize how transmission reliability affects the perceptual quality of the regenerated signal. Denote the perception-error function as $P_{\text{forward}}(\{\psi_{ij}\}_{i,j}|R)$ for uncoded forward-with-error scheme and $P_{\text{discard}}(\{\Psi_i\}_i|R)$ for coded discard-with-error scheme. Based on Lemma 1 and Lemma 2, the following corollary is established.

Corollary 1. *$P_{\text{forward}}(\{\psi_{ij}\}_{i,j}|R)$ and $P_{\text{discard}}(\{\Psi_i\}_i|R)$ are non-decreasing with ψ_{ij} and Ψ_i , respectively. This monotonic relationship demonstrates that the perceptual quality of the regenerated signal deteriorates as transmission errors increase.*

C. Semantic Value

Based on the previously analyzed perception-error functions, we define semantic values for both transmitted and received semantic data streams to quantify their semantic similarities with the original source signal.

Definition 1. The semantic value of the i -th transmitted semantic data stream \mathbf{K}_i is defined as:

$$L_i = 1 - P^{(i)}, \quad (16)$$

where $P^{(i)} = \delta(P_{\mathbf{X}}, P_{\mathbf{X}^{(i)}})$ is the perception value of regenerated signal $\mathbf{X}^{(i)} = \mathcal{F}_{\text{dec}}(\mathbf{K}_i)$ synthesized using the i -th semantic data stream \mathbf{K}_i .

Definition 2. The semantic values of the i -th received semantic data stream $\hat{\mathbf{K}}_i$ under the uncoded forward-with-error and coded discard-with-error schemes are defined as:

$$\hat{L}_{i,\text{forward}}(\{\psi_{ij}\}_j) = 1 - P_{\text{forward}}^{(i)}(\{\psi_{ij}\}_j), \quad (17)$$

and

$$\hat{L}_{i,\text{discard}}(\Psi_i) = 1 - P_{\text{discard}}^{(i)}(\Psi_i), \quad (18)$$

where $P_{\text{forward}}^{(i)}(\{\psi_{ij}\}_j) = \delta(P_{\mathbf{X}}, P_{\hat{\mathbf{X}}^{(i)}})$ is the perception value of the regenerated signal $\hat{\mathbf{X}}^{(i)} = \mathcal{F}_{\text{dec}}(\hat{\mathbf{K}}_i)$ synthesized using the i -th received semantic data stream $\hat{\mathbf{K}}_i$ with BER ψ_{ij} . $P_{\text{discard}}^{(i)}(\Psi_i) = \Psi_i \delta(P_{\mathbf{X}}, P_{\hat{\mathbf{X}}_0}) + (1 - \Psi_i) \delta(P_{\mathbf{X}}, P_{\mathbf{X}^{(i)}})$ where $\delta(P_{\mathbf{X}}, P_{\hat{\mathbf{X}}_0}) = 1$.

Remark 1. The semantic value of the received semantic data stream is non-increasing in ψ_{ij} or Ψ_i , indicating that transmission errors result in loss of semantic information.

Remark 2. The semantic values differ among the semantic data streams, reflecting their varying levels of importance in signal regeneration.

Remark 3. For any given semantic data stream, its semantic value varies across different perceptual measurements, implying that its importance is related to the specific tasks or goals at the receiver.

IV. PROBLEM FORMULATIONS

This section investigates the semantic-aware power allocation problems for both uncoded forward-with-error and coded discard-with-error schemes, aiming to minimize total power consumption while maintaining semantic performance. Given that ultra-low rates are achievable in generative SemCom systems, we focus on highly reliable transmission using uncoded BPSK and finite blocklength coding [24].

Let \mathbf{z}_i be the transmitted signal of the i -th semantic data stream such that $\mathbb{E}\{\mathbf{z}_i^H \mathbf{z}_i\} = Z_i$, where Z_i is the length of the transmitted signal. The i -th received semantic signal can be written as:

$$\mathbf{y}_i = h_i \sqrt{q_i} \mathbf{z}_i + \mathbf{n}_i, \quad (19)$$

where h_i is the block-fading channel. \mathbf{n}_i is the Gaussian noise vector, with each element following the distribution of $\mathcal{CN}(0, \sigma_i^2)$. q_i is the allocated power for the i -th semantic data stream. The signal-to-noise-ratio (SNR) is given by:

$$\text{snr}_i = \frac{q_i |h_i|^2}{\sigma_i^2}. \quad (20)$$

Under the channel-uncoded case with BPSK modulation, the length of the transmit signal satisfies $Z_i = K_i$. The total power consumption is given by $\sum_{i=1}^I K_i q_i$. The BER is uniform across all bits under the block-fading channel, i.e., $\psi_{ij} = \psi_i, \forall j = 1, \dots, K_i$, which is expressed as:

$$\psi_i = Q(\sqrt{2\text{snr}_i}), \quad (21)$$

where $Q(x) = \frac{1}{\sqrt{2\pi}} \int_x^\infty e^{-\frac{u^2}{2}} du$ is the Q-function. The probability of $\hat{\mathbf{K}}_i$ conditioning on \mathbf{K}_i is yielded by $\mathbb{P}(\hat{\mathbf{K}}_i | \mathbf{K}_i) = (\psi_i)^{k_i} (1 - \psi_i)^{K_i - k_i}$, where k_i is the number of incorrect bits. To minimize total power consumption while ensuring the semantic performance, the problem is formulated as

$$(\mathcal{P}1) : \min_{q_i} \sum_{i=1}^I K_i q_i \quad (22a)$$

$$\text{s.t. } P_{\text{forward}}(\{\psi_i\}_i) \leq \bar{P} \quad (22b)$$

$$\psi_i = Q(\sqrt{2\text{snr}_i}), \forall i \in \mathcal{I} \quad (22c)$$

where \bar{P} represents the maximum tolerate perceptual distance.

Under the channel-coded case employing finite blocklength coding, the length of transmit signal Z_i equals the channel codeword length N_i , where $N_i \geq K_i$. The coding rate is given by $K_i/N_i \leq 1$, and the total power equals $\sum_{i=1}^I N_i q_i$. According to [24], the BLER of the i -th semantic data stream is lower bounded by:

$$\Psi_i = Q\left(\ln 2 \sqrt{\frac{N_i}{V_i}} \left(C_i - \frac{K_i}{N_i}\right)\right), \quad (23)$$

where C_i is the channel capacity expressed as $C_i = \log_2(1 + \text{snr}_i)$, V_i is the channel dispersion expressed as $V_i = 1 - (1 + \text{snr}_i)^{-2}$. Using this BLER bound, the problem

that minimizes total power consumption while ensuring the semantic performance, is formulated as

$$(\mathcal{P}2) : \min_{q_i} \sum_{i=1}^I N_i q_i \quad (24a)$$

$$\text{s.t. } P_{\text{discard}}(\{\Psi_i\}_i) \leq \bar{P} \quad (24b)$$

$$\Psi_i = Q\left(\ln 2 \sqrt{\frac{N_i}{V_i}} \left(C_i - \frac{K_i}{N_i}\right)\right), \forall i \in \mathcal{I}. \quad (24c)$$

While problems ($\mathcal{P}1$) and ($\mathcal{P}2$) are challenging to solve optimally due to their non-convex constraints, the following corollary is established based on Corollary 1.

Corollary 2. *The optimal solutions to problems ($\mathcal{P}1$) and ($\mathcal{P}2$) satisfy the equality conditions in constraints (22b) and (24b), respectively.*

Proof. The perception value is non-increasing with q_i , as both BER ψ_i and BLER Ψ_i are monotonically decreasing with q_i . Therefore, the optimal solution satisfies the perception constraints with equality. \square

V. SEMANTIC-AWARE POWER ALLOCATION

Since semantic features exhibit varying levels of importance, conventional resource allocation strategies may be inefficient. This section presents two semantic-aware power allocation methods: a proportional method that decouples the perception constraint to yield a closed-form solution, and a bisection method that employs bisection search to find a locally optimal solution.

A. Semantic-Aware Proportional Method

By assuming the independent impact of semantic data streams on the perceptual quality of the regenerated signal, we decompose the perception constraint into I independent constraints on semantic values of the received data streams. Problems ($\mathcal{P}1$) and ($\mathcal{P}2$) can be relaxed into

$$(\mathcal{P}1-1) : \min_{q_i} \sum_{i=1}^I K_i q_i \quad (25a)$$

$$\text{s.t. } \hat{L}_{i,\text{forward}}(\psi_i) \geq \bar{L}_i, \forall i \in \mathcal{I}, \quad (25b)$$

$$\psi_i = Q(\sqrt{2\text{snr}_i}), \quad (25c)$$

and

$$(\mathcal{P}2-1) : \min_{q_i} \sum_{i=1}^I N_i q_i \quad (26a)$$

$$\text{s.t. } \hat{L}_{i,\text{discard}}(\Psi_i) \geq \bar{L}_i, \forall i \in \mathcal{I}, \quad (26b)$$

$$\Psi_i = Q\left(\ln 2 \sqrt{\frac{N_i}{V_i}} \left(C_i - \frac{K_i}{N_i}\right)\right), \forall i \in \mathcal{I}, \quad (26c)$$

respectively, where \bar{L}_i denotes the semantic value requirements corresponding to the semantic performance requirement \bar{P} . As stated in Remark 1, the semantic value of the received semantic data stream is non-increasing with respect to (w.r.t.) BER ψ_i or BLER Ψ_i . Consequently, the optimal solutions to (P1-1) and (P2-1) are achieved when constraints (25b) and (26b) are satisfied with equality, establishing the following theorem.

Theorem 1. For problem (P1-1), the optimal solutions q_i^* is given by:

$$q_i^* = \frac{\sigma_i^2}{2|h_i|^2} (Q^{-1}(\psi_i^*))^2, \quad (27)$$

where ψ_i^* is obtained by solving equation $\hat{L}_{i,\text{forward}}(\psi_i) = \bar{L}_i$.

For problem (P2-1), denote Ψ_i^* as the solution to $\hat{L}_{i,\text{discard}}(\Psi_i) = \bar{L}_i$, and define $\alpha_i \triangleq Q^{-1}(\Psi_i^*)/\sqrt{N_i}$. The optimal solution q_i^* is given by:

$$q_i^* = \frac{\sigma_i^2}{|h_i|^2} \left(e^{\frac{K_i}{N_i} + \eta_i^*} - 1 \right), \quad (28)$$

where $\eta_i^* = W(2\alpha_i, -2\alpha_i; -4e^{-2K_i/N_i}\alpha_i^2)/2$, with $W(\cdot)$ denoting the generalized Lambert W function¹. The proof appears in Appendix B.

B. Semantic-Aware Bisection Method

For image tasks, two semantic extractors suffice to obtain semantic features for high-quality image regeneration [35], where one extractor provides textual description while the other captures structural features. Given this dual-extractor configuration, problems (P1) and (P2) can be reformulated based on Corollary 2 as follows.

For the uncoded BPSK scheme, the allocated power derived from (21) can be expressed as $p_i = \frac{\sigma_i^2}{2|h_i|^2} (Q^{-1}(\psi_i))^2$. Thus, problem (P1) with dual-extractor configuration is reduced into:

$$(\mathcal{P1-2}) : \quad \min_{\psi_1, \psi_2} \sum_{i=1}^2 \frac{K_i \sigma_i^2}{2|h_i|^2} (Q^{-1}(\psi_i))^2 \quad (29a)$$

$$\text{s.t.} \quad P_{\text{forward}}(\psi_1, \psi_2) = \bar{P}. \quad (29b)$$

For the finite blocklength coding scheme, the allocated power derived from (23) is given by $p_i = \frac{\sigma_i^2}{|h_i|^2} \text{snr}_i(\Psi_i)$, where $\text{snr}_i(\Psi_i)$ is the solution to equation (23). Accordingly, problem (P2) with dual-extractor configuration is reduced into:

$$(\mathcal{P2-2}) : \quad \min_{\Psi_1, \Psi_2} \sum_{i=1}^2 \frac{N_i \sigma_i^2}{|h_i|^2} \text{snr}_i(\Psi_i) \quad (30a)$$

$$\text{s.t.} \quad P_{\text{discard}}(\Psi_1, \Psi_2) = \bar{P}. \quad (30b)$$

¹The generalized Lambert W function $W(t_1, t_2; a)$ is the solution to the transcendental equation $(x - t_1)(x - t_2)e^x = a$ [34].

Algorithm 1 Semantic-Aware Bisection Method for Semantic Encoder with Dual-Extractor Configuration

Input: $(\Phi_1^L, \Phi_2^L), (\Phi_1^R, \Phi_2^R)$.

Output: (Φ_1, Φ_2) .

- 1: Compute partial gradients $(\frac{\partial f}{\partial \Phi_1^L}, \frac{\partial f}{\partial \Phi_2^L})$ and $(\frac{\partial f}{\partial \Phi_1^R}, \frac{\partial f}{\partial \Phi_2^R})$.
 - 2: Compute gradients $\nabla_{\Phi_1^L} \Phi_2^L$ and $\nabla_{\Phi_1^R} \Phi_2^R$ by implicit differentiation of (29b) or (30b).
 - 3: **if** $\frac{\partial f}{\partial \Phi_1^L} + \nabla_{\Phi_1^L} \Phi_2^L \frac{\partial f}{\partial \Phi_2^L} \geq 0$.
 - 4: $(\Phi_1, \Phi_2) \leftarrow (\Phi_1^L, \Phi_2^L)$.
 - 5: **else if** $\frac{\partial f}{\partial \Phi_1^R} + \nabla_{\Phi_1^R} \Phi_2^R \frac{\partial f}{\partial \Phi_2^R} \leq 0$
 - 6: $(\Phi_1, \Phi_2) \leftarrow (\Phi_1^R, \Phi_2^R)$.
 - 7: **else**
 - 8: **while** $\Phi_1^R - \Phi_1^L \geq \epsilon$
 - 9: $\Phi_1 = (\Phi_1^R + \Phi_1^L)/2$.
 - 10: Obtain Φ_2 by solve the equation (29b) or (30b).
 - 11: Compute partial gradients $(\frac{\partial f}{\partial \Phi_1}, \frac{\partial f}{\partial \Phi_2})$ and $\nabla_{\Phi_1} \Phi_2$.
 - 12: **if** $\frac{\partial f}{\partial \Phi_1} + \nabla_{\Phi_1} \Phi_2 \frac{\partial f}{\partial \Phi_2} \geq 0$.
 - 13: $(\Phi_1^R, \Phi_2^R) \leftarrow (\Phi_1, \Phi_2)$.
 - 14: **else**
 - 15: $(\Phi_1^L, \Phi_2^L) \leftarrow (\Phi_1, \Phi_2)$.
 - 16: **end**
 - 17: **end**
 - 18: **end**
-

The local optimal solution can be obtained through bisection search by locating where the objective function gradient equals zero. For simplicity of notation, denote (Φ_1, Φ_2) ($\Phi_1 \in \{\psi_1, \Psi_1\}$, $\Phi_2 \in \{\psi_2, \Psi_2\}$) as the optimizing variables, and f ($f \in \{f_1, f_2\}$) as the objective functions of the above problems. The feasible solutions (Φ_1, Φ_2) forms a line on the perception-error surfaces. For any two feasible solutions $(\Phi_1^{(1)}, \Phi_2^{(1)})$ and $(\Phi_1^{(2)}, \Phi_2^{(2)})$, we have $\Phi_2^{(2)} \leq \Phi_2^{(1)}$ if $\Phi_1^{(1)} \geq \Phi_1^{(2)}$. Denoting the line endpoints as (Φ_1^L, Φ_2^L) and (Φ_1^R, Φ_2^R) , where $\Phi_1^R \geq \Phi_1^L$, the procedure to obtain the local optimal solution is summarized in Algorithm 1.

VI. SIMULATION RESULTS

This section considers the image task and focuses on three key aspects: 1). Validating the effectiveness of the proposed generative SemCom framework; 2). Verifying perception-error functions and the semantic values of different semantic data streams; and 3). Assessing the performance of the semantic-aware power allocation methods. For comprehensive evaluation, both CLIP and MS-SSIM metric are considered for semantic performance assessment.

A. Effectiveness of the Generative SemCom Framework

Fig. 2 illustrates the proposed generative SemCom framework for the image task. The semantic encoder utilizes two extractors: a textual prompt feature extractor using textual transform coding via prompt inversion [36], and an edge map feature extractor employing HED with NTC [37]

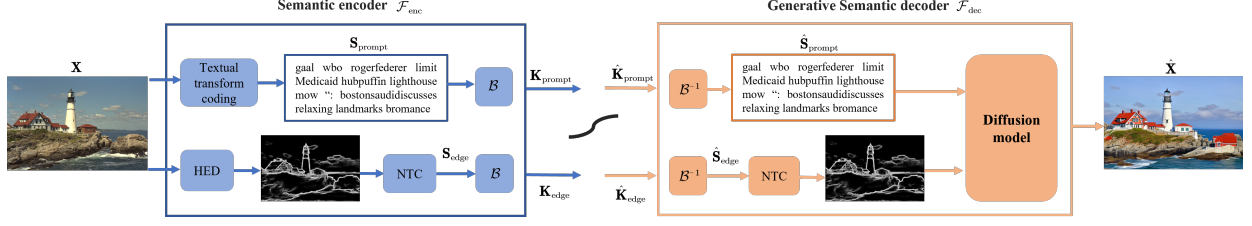


Fig. 2. The proposed generative SemCom framework for the image task with dual semantic extractors for textual prompt and edge map features.

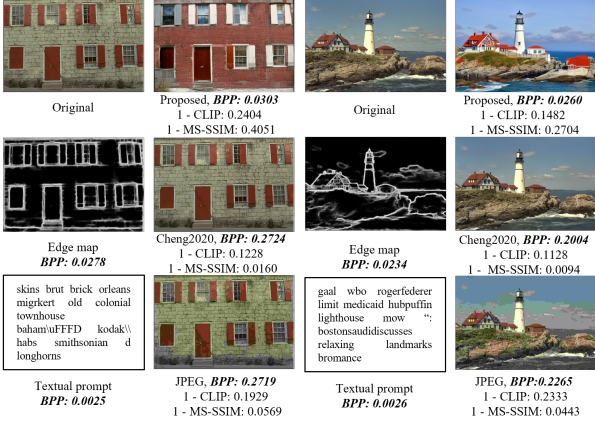


Fig. 3. Visual quality and compression rate comparison of the proposed approach against JPEG and Cheng2020.

for compression. For the semantic decoder, the pre-trained ControlNet [38] built upon the Stable Diffusion model [20] is adopted. The channel for the i -th semantic data stream is modeled as $h_i = \sqrt{P_{\text{Loss}}}\tilde{h}_i$. Here, the path loss is given by $P_{\text{Loss}} = P_{\text{Loss},0}(d/d_0)^{-\alpha}$, with distance $d = 100$ m, reference path loss $P_{\text{Loss},0} = -30$ dB at $d_0 = 1$ m, and path loss exponent $\alpha = -3.4$. \tilde{h}_i is Rayleigh fading channel with a variance of 1. The noise power is set to $\sigma_i^2 = -110$ dBm. The coding rate is set to $K_i/N_i = 0.8$ for the coded discard-with-error scheme. Due to the complexity of deriving explicit perception-error functions, numerical simulations are conducted using the Kodak dataset [39]. For notation simplicity, we occasionally use subscripts 1 and 2 to represent the textual prompt and edge map features, respectively.

Fig. 3 illustrates the regenerated images using the proposed generative SemCom framework, compared against traditional JPEG [40] and the deep learning-based Cheng2020 [41] compression approaches. The compression rate is measured by bit per pixel (bpp). The results demonstrate that our approach achieves significantly lower compression rates (0.0303 bpp and 0.0260 bpp) in the two example images, outperforming both JPEG (0.2719 bpp and 0.2265 bpp) and Cheng2020 (0.2724 bpp and 0.2004 bpp) by approximately a factor of 10. This significant compression improvement maintains comparable perceptual quality, particularly when evaluated

using the CLIP metric. These visual results validate the effectiveness of the proposed generative SemCom framework in achieving ultra-low rate while preserving semantics. For comprehensive evaluation of transmission reliability effects, Fig. 10 in Appendix C presents additional regenerated images across varying BER ψ_i and BLER Ψ_i . It shows that showing that the visual qualities of the regenerated images are degrading with transmission errors. Moreover, the results under the coded discard-with-error scheme demonstrate that the textual prompt feature better provides the semantic contents while the edge map captures the structural similarity.

B. Perception-Error Function and Semantic Value

Fig. 4 illustrates the perception-error functions and semantic values of data streams for both uncoded forward-with-error and coded discard-with-error schemes. For the uncoded forward-with-error scheme, the perception-error functions are derived through curve fitting of numerical simulation data shown as dots. Without transmission errors, both schemes achieve the best-case perception values (P_{best}), which are 0.3191 and 0.3313 for CLIP, and MS-SSIM metrics, respectively. With maximum transmission errors, the worst-case values (P_{worst}) reach 0.8112 for the CLIP and 0.4720 for the MS-SSIM metrics under the uncoded scheme, and 1 under the coded scheme. As the increase of BERs and BLERs, the perception qualities of the regenerated images are degraded, confirming Corollary 1. Notably, prompt features demonstrate stronger influence on CLIP performance, while edge map features show greater impact on MS-SSIM metrics, as CLIP measures similarity in high-level meaning while MS-SSIM captures spatial structural similarity. In addition, the edge map feature is more vulnerable to BER than the textual prompt feature, due to further NTC compression and larger data stream length.

The semantic values are also decreasing with BERs or BLERs. For the CLIP metric, textual prompt and edge map data streams show semantic values of $L_1 = 0.5887$ and $L_2 = 0.3596$ respectively, while for the MS-SSIM metric, they show values of $L_1 = 0.5465$ and $L_2 = 0.6355$. The relationship $L_1 + L_2 > 1 - P_{\text{best}}$ indicates that prompt and edge map semantic features are not semantically independent. The behavior of semantic values differs between the two error-handling schemes. Fig. 4(c) shows that under uncoded

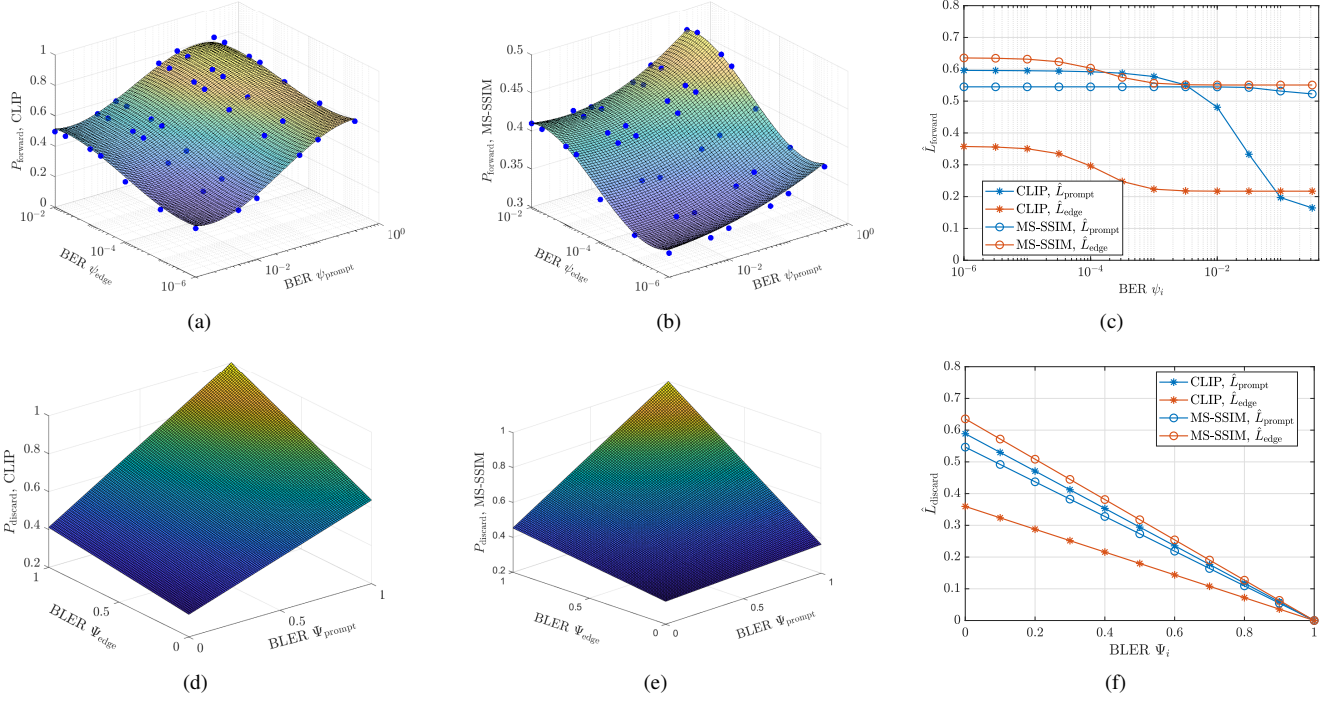


Fig. 4. The perception-error functions and semantic values: (a-c). Uncoded forward-with-error scheme. (e-f). Coded discard-with-error scheme.

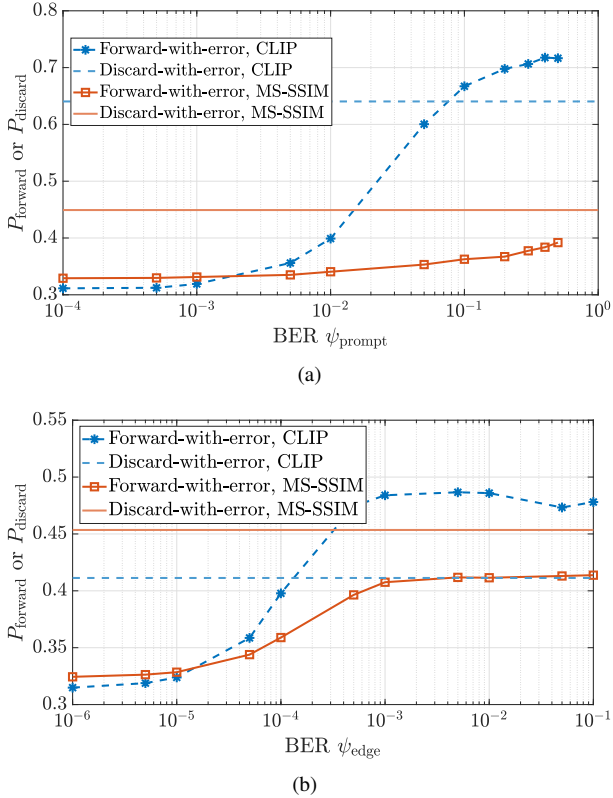


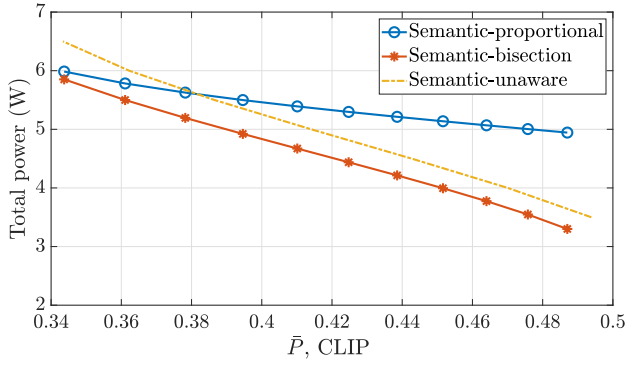
Fig. 5. The perception-error functions in the case where one of semantic features is correctly received.

forward-with-error scheme, the received semantic data streams maintain positive semantic values even at maximum BER. However, the semantic values under coded discard-with-error scheme approach 0 as BLER nears 1 as shown in Fig. 4(f), as the semantic decoder becomes inactive when all received streams contain errors and are discarded. Fig. 5 shows the perception-error functions in the case of one correctly received semantic feature, revealing that forwarding additional semantic data stream with high BER degrades semantic performance compared to discarding them at the decoder. This finding validates the proposed discard-with-error scheme.

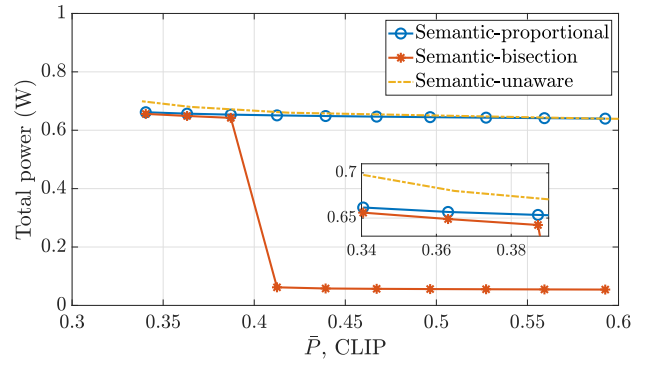
C. Performance Assessment

To assess the proposed semantic-aware power allocation methods, we compare them against conventional semantic-unaware approaches in terms of the total power consumption, transmission error and channel capacity. The proposed and traditional baseline methods are listed as follows:

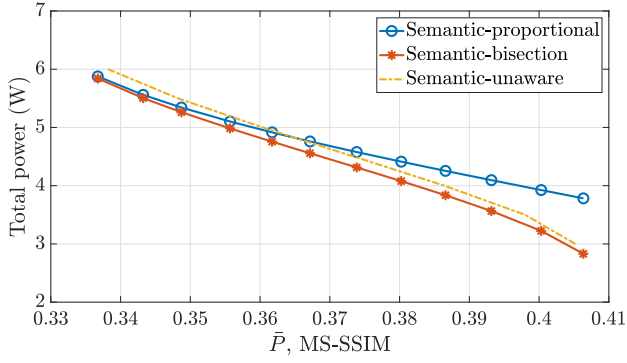
- Semantic-proportional: The allocated power is obtained based on Theorem 1, where semantic value requirements satisfy $\bar{L}_i/L_i = \bar{L}_j/L_j, \forall i, j \in \mathcal{I}$.
- Semantic-bisection: The allocated power is obtained based on Algorithm 1.
- Semantic-unaware: The allocated power is obtained to ensure equal SNRs for all semantic data streams, resulting in identical BER and capacity performance under the channel-uncoded case, and identical capacity under the channel-coded case.



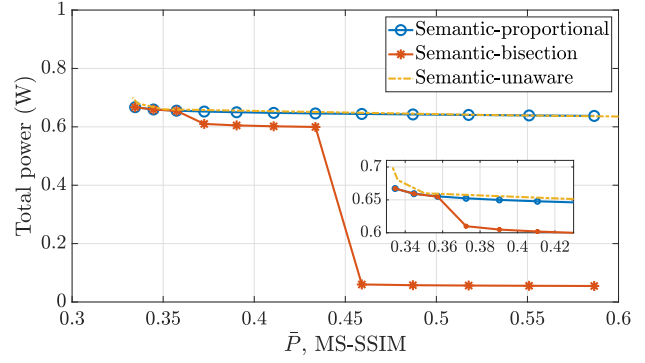
(a)



(b)

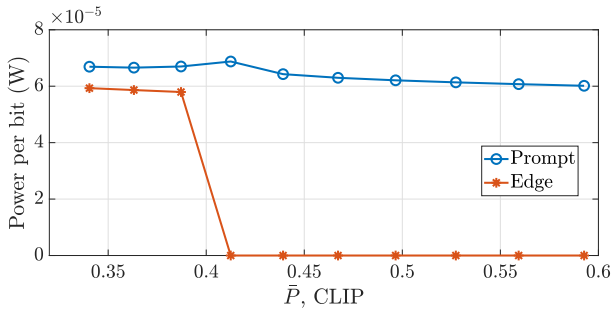


(c)

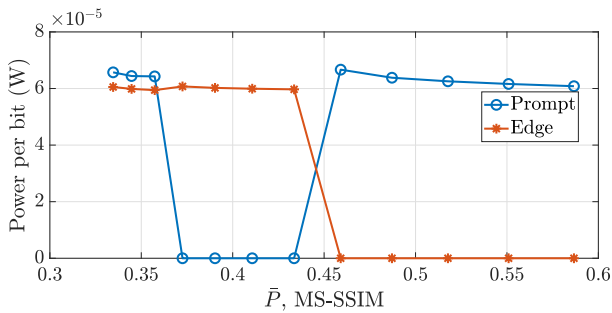


(d)

Fig. 6. Comparisons of total power consumption. (a). Uncoded forward-with-error with the CLIP metric. (b) Coded discard-with-error with the CLIP metric. (c). Uncoded forward-with-error with the MS-SSIM metric. (d) Coded discard-with-error with the MS-SSIM metric.



(a)



(b)

Fig. 7. Average power per bit: (a). Coded discard-with-error scheme with the CLIP metric. (b). Coded discard-with-error scheme with the MS-SSIM metric.

Fig. 6 compares total power consumption under specified perception performance requirements. The proposed semantic-bisection method achieves significant power savings compared to the baseline: up to 10% in channel-uncoded cases and 90% in channel-coded cases. Under stringent semantic requirements, the semantic-proportional method achieves similar performance to the semantic-bisection method. However, its advantage over the semantic-unaware method diminishes as \bar{P} increases. In the channel-coded case, the semantic-bisection method shows sharp power reductions at a certain semantic requirement \bar{P} , corresponding to when power allocation to one semantic stream becomes zero as illustrated in Fig. 7. While the edge map feature shows higher semantic similarity under the MS-SSIM metric than the prompt, the prompt feature proves more valuable when considering semantic information per bit due to its shorter length. This leads to prioritizing prompt transmission at high \bar{P} . However, in the range of $0.3313 \leq \bar{P} \leq 0.4720$, the prompt feature is not transmitted as it alone cannot meet such requirements.

Fig. 8 compares transmission error and channel capacity performance under specified CLIP perception performance requirements. Under the semantic-unaware method, prompt and edge semantic data streams achieve identical capacities in both channel-uncoded and channel-coded cases due to

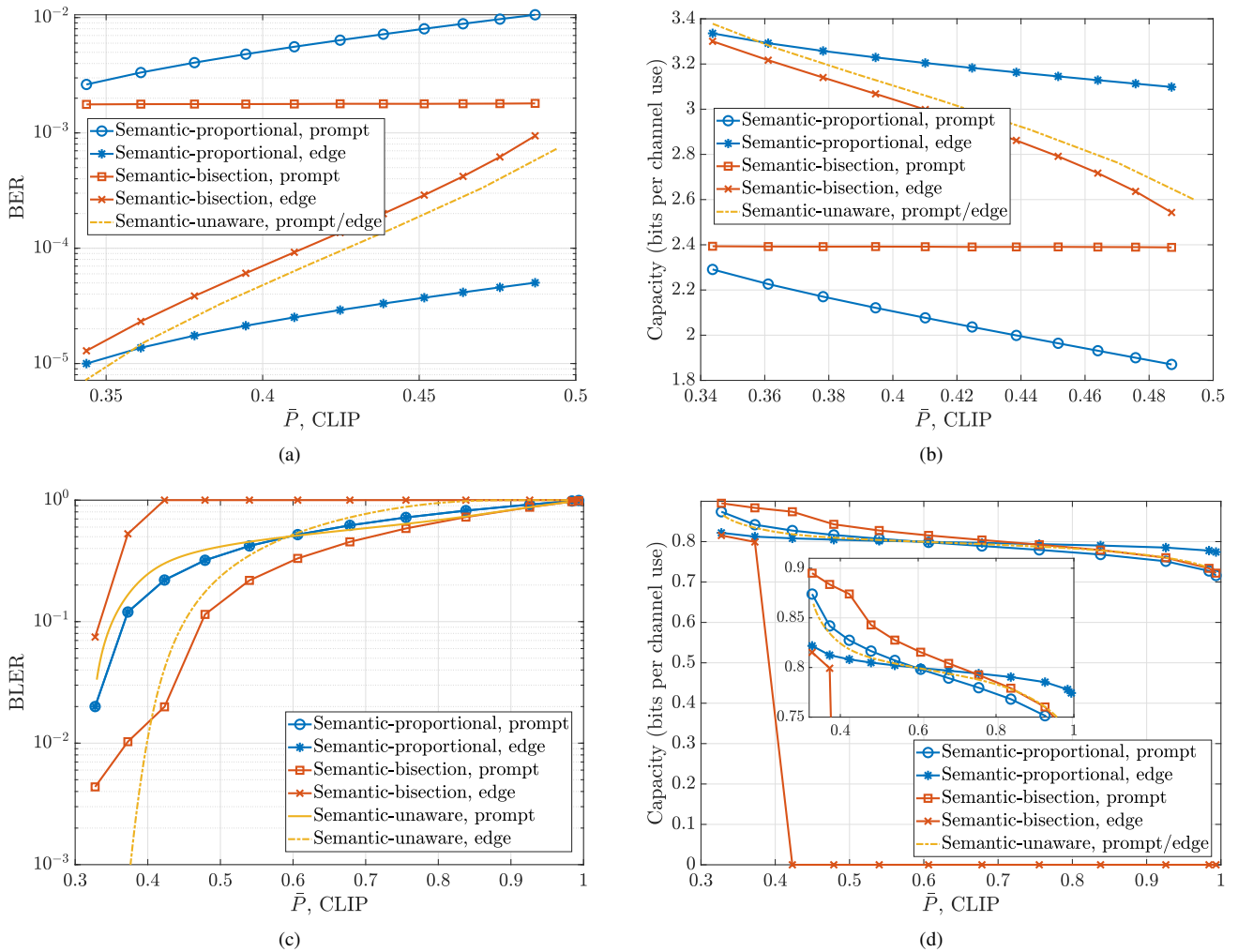


Fig. 8. Comparisons of transmission error and capacity: (a). BER under uncoded forward-with-error scheme. (b). Capacity under uncoded forward-with-error scheme. (c). BLER under coded discard-with-error scheme. (d). Capacity under discard-with-error schemes.

equal received SNRs. While their BERs are identical in the channel-uncoded case, BLERs differ in the channel-coded case due to their varying sequence lengths. For the channel-uncoded case, the semantic-unaware method achieves lower BERs and higher capacities, as it requires higher power consumption to obtain the required semantic performance \bar{P} . Compared to the semantic-proportional method, it exhibits higher BER and lower capacity for edge feature transmission. In the channel-coded case, the semantic-proportional method achieves identical BLERs for both features due to the setting of $\bar{L}_i/L_i = \bar{L}_j/L_j, \forall i, j \in \mathcal{I}$. The semantic-unaware method shows lower BLER and higher capacity for edge feature transmission compared to semantic-bisection methods, with opposite results for the prompt feature. When \bar{P} exceeds a threshold, edge map transmission shows BLER of 1 and capacity of 0, indicating no power allocation. These results suggest selective feature transmission based on channel conditions can optimize resource usage, potentially enabling adaptive semantic coding rates through selective semantic

extractor activation. This is further supported by Fig. 9, which shows the cumulative distribution function (CDF) of semantic performance across various power budgets in the channel-coded case.

VII. CONCLUSION

This paper presented a generative SemCom framework using pre-trained foundation models, where uncoded forward-with-error and coded discard-with-error schemes were proposed for the semantic decoder. The relationship between transmission reliability and regenerated signal quality was characterized through rate-distortion-perception theory, enabling semantic value quantification of semantic similarity between semantic data streams and the original source. Semantic-aware power allocation methods were developed for ultra-low rate and high fidelity SemComs to minimize power consumption while maintaining semantic performance. Simulations on the Kodak dataset validated the effectiveness of the proposed generative SemCom framework and verified the

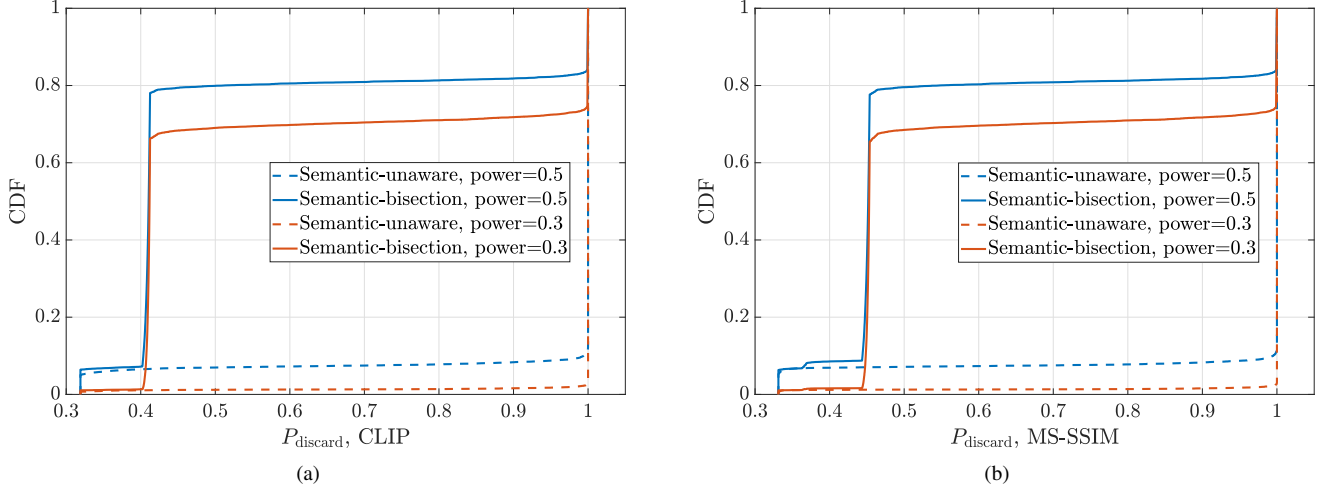


Fig. 9. CDF of the achieved perception value under the coded discard-with-error scheme: (a). CLIP metric. (b). MS-SSIM metric.

perception-error functions and semantic values. The proposed semantic-aware method was demonstrated to outperform the conventional approach, particularly in the channel-coded case. A key finding revealed that power allocated to certain semantic data streams could be zero, suggesting potential computation savings through selective deactivation of semantic extractors. This insight points toward future research in adaptive semantic communications with channel feedback to improve both radio and computation efficiency.

APPENDIX A PROOF OF LEMMA 2

Proof. According to the chain rule of mutual information [33], $I(\mathbf{K}; \hat{\mathbf{K}})$ under uncoded forward-with-error scheme satisfies:

$$\begin{aligned} I(\mathbf{K}_i; \hat{\mathbf{K}}_i) &= \sum_{j=1}^{K_i} I(\mathbf{K}_{ij}; \hat{\mathbf{K}}_i | \mathbf{K}_{i1}, \dots, \mathbf{K}_{i(j-1)}) \\ &= \sum_{j=1}^{K_i} I(\mathbf{K}_{ij}; \hat{\mathbf{K}}_i) \end{aligned} \quad (31)$$

where the second equality holds due to bit independence as per Assumption 1. Further applying the chain rule to $I(\mathbf{K}_{ij}; \hat{\mathbf{K}}_i)$ yields:

$$\begin{aligned} I(\mathbf{K}_{ij}; \hat{\mathbf{K}}_i) &= \sum_{j'=1}^{K_i} I(\mathbf{K}_{ij}; \hat{\mathbf{K}}_{ij'} | \hat{\mathbf{K}}_{i1}, \dots, \hat{\mathbf{K}}_{i(j'-1)}) \\ &= \sum_{j'=1}^{K_i} I(\mathbf{K}_{ij}; \hat{\mathbf{K}}_{ij'}) \\ &= I(\mathbf{K}_{ij}; \hat{\mathbf{K}}_{ij}), \end{aligned} \quad (32)$$

where the second equality follows from the interdependence among received bits within $\hat{\mathbf{K}}_i$, and the third equality holds because received bit $\hat{\mathbf{K}}_{ij'}$ is independent of $\hat{\mathbf{K}}_{ij}$ when $j' \neq j$.

Given that $I(\mathbf{K}_{ij}; \hat{\mathbf{K}}_{ij}) = H(\phi_{ij}) - H(\psi_{ij})$ for a Bernoulli source transmitted over binary symmetric channels, we obtain:

$$I(\mathbf{K}_i; \hat{\mathbf{K}}_i) = \sum_{j=1}^{K_i} H(\phi_{ij}) - H(\psi_{ij}), \quad (33)$$

which decreases in BER ψ_{ij} with $\psi_{ij} \leq 0.5$.

For the coded discard-with-error scheme, since erroneous received data streams are discarded, we have $H(\mathbf{K}_i | \hat{\mathbf{K}}_i \neq \mathbf{K}_i) = H(\mathbf{K}_i)$. Consequently, the mutual information $I(\mathbf{K}; \hat{\mathbf{K}})$ can be expressed as:

$$\begin{aligned} I(\mathbf{K}_i; \hat{\mathbf{K}}_i) &= H(\mathbf{K}_i) - H(\mathbf{K}_i | \hat{\mathbf{K}}_i) \\ &= H(\mathbf{K}_i) - \mathbb{P}(\hat{\mathbf{K}}_i = \mathbf{K}_i) H(\mathbf{K}_i | \hat{\mathbf{K}}_i = \mathbf{K}_i) \\ &\quad - P(\hat{\mathbf{K}}_i \neq \mathbf{K}_i) H(\mathbf{K}_i | \hat{\mathbf{K}}_i \neq \mathbf{K}_i) \\ &= H(\Phi_i) - \Psi_i H(\Phi_i), \end{aligned} \quad (34)$$

which decreases with the BLER Ψ_i . The proof is thus completed. \square

APPENDIX B PROOF OF LEMMA 1

Proof. The solutions to problems $\mathcal{P}1$ -1 and $\mathcal{P}2$ -1 can be readily obtained by substituting ψ_i^* and Ψ_i^* back to (21) and (23). The difficulty in obtaining the optimal power allocation to problem $\mathcal{P}3$ -1 lies in the transcendental equation of (23). Letting $\alpha_i \triangleq \frac{Q^{-1}(\Psi_i^*)}{\sqrt{N_i}}$, (23) can be rewritten as

$$\ln \left((1 + \text{snr}_i) e^{-\frac{K_i}{N_i}} \right) - \alpha_i \sqrt{1 - (1 + \text{snr}_i)^{-2}} = 0. \quad (35)$$

Letting $\eta_i \triangleq \ln \left((1 + \text{snr}_i) e^{-K_i/N_i} \right)$ and $\beta_i = e^{-K_i/N_i}$, we have $1 + \text{SNR}_i = \beta_i^{-1} e_i^\eta$. (35) can then be further rewritten by

$$\eta_i = \alpha_i \sqrt{1 - \beta_i^2 e^{-2\eta_i}}, \quad (36)$$

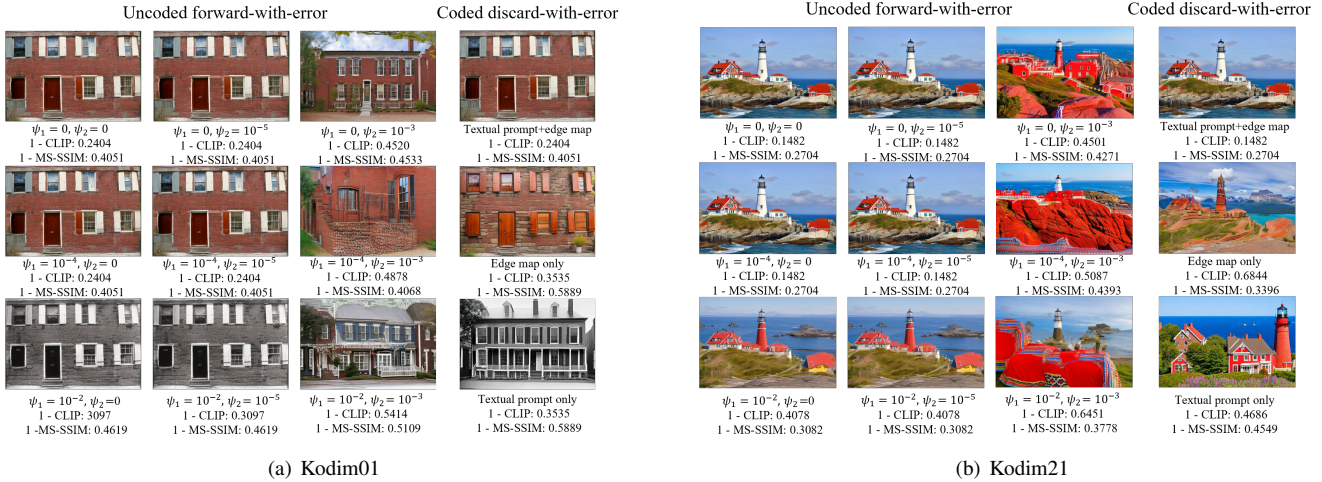


Fig. 10. Regenerated images under uncoded forward-with-error and coded discard-with-error schemes: (a). Kodim01. (b). Kodim21.

which can be further expressed in a generalized Lambert W function fashion by

$$-4\beta_i^2\alpha_i^2 = (2\eta_i - 2\alpha_i)(2\eta_i + 2\alpha_i)e^{2\eta_i}. \quad (37)$$

The solution of η_i^* is denoted as $\eta_i^* = W(2\alpha_i, -2\alpha_i; -4\beta_i^2\alpha_i^2)/2$. Thus, the optimal power q_i^* is given by

$$q_i^* = \frac{\sigma_i^2}{2|h_i|^2} \left(e^{\frac{K_i}{N_i} + \eta_i^*} - 1 \right). \quad (38)$$

□

APPENDIX C

VISUAL QUALITY OF THE REGENERATED IMAGES

Fig. 10 depicts the regenerated images of Kodim01 and Kodim21 with transmission errors. The left three columns are the regenerated images under the uncoded forward-with-error scheme, while the rightmost column shows the regenerated images under the coded discard-with-error scheme.

REFERENCES

- [1] R. Carnap, Y. Bar-Hillel *et al.*, “An outline of a theory of semantic information,” Res. Lab. Electron., Massachusetts Inst. Technol., Cambridge MA, USA, Tech. Rep. Tech. Rep. 247, Oct. 1952.
- [2] D. Gündüz, Z. Qin, I. E. Aguerri, H. S. Dhillon, Z. Yang, A. Yener, K. K. Wong, and C.-B. Chae, “Beyond transmitting bits: Context, semantics, and task-oriented communications,” *IEEE J. Sel. Areas Commun.*, vol. 41, no. 1, pp. 5–41, 2022.
- [3] J. Bao, P. Basu, M. Dean, C. Partridge, A. Swami, W. Leland, and J. A. Hendlar, “Towards a theory of semantic communication,” in *Proc. IEEE Net. Sci. Workshop*, West Point, NY, USA, Sept. 2011, pp. 110–117.
- [4] A. De Luca and S. Termini, “A definition of a nonprobabilistic entropy in the setting of fuzzy sets theory,” *Inf. Control*, pp. 301–312, 1971.
- [5] —, “Entropy of L-fuzzy sets,” *Inf. Control*, vol. 24, no. 1, pp. 55–73, 1974.
- [6] J. Liu, W. Zhang, and H. V. Poor, “A rate-distortion framework for characterizing semantic information,” in *Proc. IEEE Int. Symposium Inf. Theory (ISIT)*. IEEE, 2021, pp. 2894–2899.
- [7] T. Guo, Y. Wang, J. Han, H. Wu, B. Bai, and W. Han, “Semantic compression with side information: A rate-distortion perspective,” *arXiv preprint arXiv:2208.06094*, 2022.
- [8] K. Niu and P. Zhang, “A Mathematical Theory of Semantic Communication,” *J. Commun.*, vol. 45, no. 6, pp. 7–59, 2024.
- [9] Shao, Yulin and Cao, Qi and Gündüz, Deniz, “A Theory of Semantic Communication,” *IEEE Trans. Mob. Comput.*, vol. 23, no. 12, pp. 12 211–12 228, 2024.
- [10] Y. Blau and T. Michaeli, “Rethinking lossy compression: The rate-distortion-perception tradeoff,” in *Proc. Int. Conf. Machine Learning (ICML)*, Long Beach, California, USA, Jun. 2019, pp. 675–685.
- [11] E. Boursoulatzé, D. B. Kurka, and D. Gündüz, “Deep joint source-channel coding for wireless image transmission,” *IEEE Trans. Cognitive Commun. Networking*, vol. 5, no. 3, pp. 567–579, 2019.
- [12] H. Xie, Z. Qin, G. Y. Li, and B.-H. Juang, “Deep learning enabled semantic communication systems,” *IEEE Trans. Signal Process.*, vol. 69, pp. 2663–2675, 2021.
- [13] Z. Weng and Z. Qin, “Semantic communication systems for speech transmission,” *IEEE J. Sel. Areas Commun.*, vol. 39, no. 8, pp. 2434–2444, 2021.
- [14] T.-Y. Tung and D. Gündüz, “Deepwive: Deep-learning-aided wireless video transmission,” *IEEE J. Sel. Areas Commun.*, vol. 40, no. 9, pp. 2570–2583, 2022.
- [15] M. Yang, C. Bian, and H.-S. Kim, “OFDM-guided deep joint source channel coding for wireless multipath fading channels,” *IEEE Trans. Cogn. Commun. Netw.*, vol. 8, no. 2, pp. 584–599, 2022.
- [16] C. Liang, H. Du, Y. Sun, D. Niyato, J. Kang, D. Zhao, and M. A. Imran, “Generative AI-driven semantic communication networks: Architecture, technologies and applications,” *IEEE Trans. Cogn. Commun. Netw.*, Jul. 2024.
- [17] K. Choi, K. Tatwawadi, A. Grover, T. Weissman, and S. Ermon, “Neural joint source-channel coding,” in *Int. Conf. Machine Learning*, Long Beach, California, USA, Jun. 2019, pp. 1182–1192.
- [18] E. Erdemir, T.-Y. Tung, P. L. Dragotti, and D. Gündüz, “Generative joint source-channel coding for semantic image transmission,” *IEEE J. Sel. Areas Commun.*, vol. 41, no. 8, pp. 2645–2657, 2023.
- [19] H. Tong, H. Li, H. Du, Z. Yang, C. Yin, and D. Niyato, “Multimodal Semantic Communication for Generative Audio-Driven Video Conferencing,” *IEEE Wireless Commun. Lett.*, 2024.
- [20] R. Rombach, A. Blattmann, D. Lorenz, P. Esser, and B. Ommer, “High-resolution image synthesis with latent diffusion models,” in *Proc. IEEE/CVF Conf. Comput. Vis. Pattern Recognit.*, New Orleans, Louisiana, Jun. 2022, pp. 10 684–10 695.
- [21] D. Ghosal, N. Majumder, A. Mehrish, and S. Poria, “Text-to-audio generation using instruction-tuned LLM and latent diffusion model,” *arXiv preprint arXiv:2304.13731*, 2023.
- [22] O. Bar-Tal, H. Chefer, O. Tov, C. Herrmann, R. Paiss, S. Zada, A. Ephrat, J. Hur, Y. Li, T. Michaeli *et al.*, “Lumiere: A space-time diffusion model for video generation,” *arXiv preprint arXiv:2401.12945*, 2024.
- [23] E. Grassucci, S. Barbarossa, and D. Comminiello, “Generative semantic

- communication: Diffusion models beyond bit recovery,” *arXiv preprint arXiv:2306.04321*, 2023.
- [24] Y. Polyanskiy, H. V. Poor, and S. Verdú, “Channel coding rate in the finite blocklength regime,” *IEEE Trans. Inf. Theory*, vol. 56, no. 5, pp. 2307–2359, 2010.
- [25] J. Li, D. Li, C. Xiong, and S. Hoi, “BLIP: Bootstrapping language-image pre-training for unified vision-language understanding and generation,” in *Proc. Int. Conf. Machine Learning (ICML)*, Baltimore, Maryland USA, Jul. 2022, pp. 12 888–12 900.
- [26] T. Weissman, “Toward textual transform coding,” *IEEE BITS Inf. Theory Mag.*, vol. 3, no. 2, pp. 32–40, 2023.
- [27] S. Xie and Z. Tu, “Holistically-nested edge detection,” in *Proc. Int. Conf. Computer Vision (ICCV)*, Santiago, Chile, Dec. 2015, pp. 1395–1403.
- [28] L.-C. Chen, G. Papandreou, I. Kokkinos, K. Murphy, and A. L. Yuille, “Deeplab: Semantic image segmentation with deep convolutional nets, atrous convolution, and fully connected crfs,” *IEEE Trans. Pattern Analysis Machine Intelligence*, vol. 40, no. 4, pp. 834–848, 2017.
- [29] J. Chen, L. Yu, J. Wan, W. Shi, Y. Ge, and W. Tong, “On the rate-distortion-perception function,” *IEEE J. Sel. Areas Inf. Theory*, vol. 3, no. 4, pp. 664–673, 2022.
- [30] J. Wang, K. C. Chan, and C. C. Loy, “Exploring clip for assessing the look and feel of images,” in *Proc. AAAI Conf. Artif. Intell.*, vol. 37, no. 2, Feb. 2023, pp. 2555–2563.
- [31] Z. Wang, E. P. Simoncelli, and A. C. Bovik, “Multiscale structural similarity for image quality assessment,” in *Proc. Asilomar Conf. Signals, Syst. Comput.*, vol. 2, Pacific Grove, CA, USA, Nov. 2003, pp. 1398–1402.
- [32] A. Radford, J. W. Kim, C. Hallacy, A. Ramesh, G. Goh, S. Agarwal, G. Sastry, A. Askell, P. Mishkin, J. Clark *et al.*, “Learning transferable visual models from natural language supervision,” in *Proc. Int. conf. machine learning (ICML)*, Virtual, Jul. 2021, pp. 8748–8763.
- [33] M. Thomas and A. T. Joy, *Elements of information theory*. Wiley-Interscience, 2006.
- [34] I. Mező and Á. Baricz, “On the generalization of the lambert W function,” *Trans. Am. Math. Soc.*, vol. 369, no. 11, pp. 7917–7934, 2017.
- [35] E. Lei, Y. B. Uslu, H. Hassani, and S. S. Bidokhti, “Text+ sketch: Image compression at ultra low rates,” *arXiv preprint arXiv:2307.01944*, 2023.
- [36] Y. Wen, N. Jain, J. Kirchenbauer, M. Goldblum, J. Geiping, and T. Goldstein, “Hard prompts made easy: Gradient-based discrete optimization for prompt tuning and discovery,” 2023. [Online]. Available: <https://arxiv.org/abs/2302.03668>
- [37] J. Ballé, P. A. Chou, D. Minnen, S. Singh, N. Johnston, E. Agustsson, S. J. Hwang, and G. Toderici, “Nonlinear transform coding,” *IEEE J. Sel. Topics Signal Process.*, vol. 15, no. 2, pp. 339–353, 2020.
- [38] L. Zhang, A. Rao, and M. Agrawala, “Adding conditional control to text-to-image diffusion models,” in *Proc. IEEE/CVF Int. Conf. Computer Vision (ICCV)*, Paris, France, Oct. 2023, pp. 3836–3847.
- [39] R. Franzen, “Kodak lossless true color image suite,” <https://r0k.us/graphics/kodak/>.
- [40] G. K. Wallace, “The JPEG still picture compression standard,” *IEEE IEEE Trans. Consum. Electron.*, vol. 38, no. 1, pp. xviii–xxxiv, 1992.
- [41] Z. Cheng, H. Sun, M. Takeuchi, and J. Katto, “Learned image compression with discretized gaussian mixture likelihoods and attention modules,” in *Proc. IEEE/CVF Conf. Comput. Vis. Pattern Recognit. (CVPR)*, Virtual, Jun. 2020, pp. 7939–7948.